Development of tools for advanced quench diagnostics at the LBNL Magnet Test Facility

M. Marchevsky, M. Turqueti, G. Sabbi, S. Caspi, S. Gourlay, *Lawrence Berkeley National Laboratory, Berkeley CA*

Introduction

Testing of high-field accelerator magnets aims at identifying potential causes of quenching, localizing quench origins and measuring quench propagation velocity along the coil winding. This information is essential for establishing protection limits and providing useful feedback to the magnet designers. Traditionally, quench studies are conducted using voltage taps. However, for magnets that are long or of complex geometry this approach becomes impractical due to large number of taps required to track quench propagation and difficulty of incorporating them into coils without jeopardizing magnet integrity. We develop and implement alternative methods of quench diagnostics, based on time-correlated multi-point sensing of magnetic and mechanical disturbances. The new systems have been designed and implemented within the LBNL's base program focused on canted-cosine-theta (CCT) magnet development [1].

PC board quench antenna array

Quench antennas have been used in various magnets to determine quench locations without relying on voltage taps. The CCT magnet geometry calls for the novel quench antenna design for optimized quench localization accuracy. We designed and fabricated quench antenna array that picks up current path disturbance caused by a normal zone formation when placed along the CCT cable winding. A sketch showing the antenna working principle is shown in Fig. 1. The antenna represents a linear array of 12 sensing elements, each consisting of two double-layer coils that are dipole-bucked to sense axial gradient of the perpendicular field. PCBs are 355 mm x 12 mm, and 1.5 mm thick; they have four Cu layers, with top and bottom layers comprising the coils and the internal ones used for interface wiring. Terminal pads at the PCBs are wired with a flat ribbon cable; two arrays may be interfaced at one end.

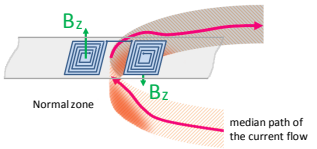

Fig. 1. A dipole-bucked coil sensor element picks up a field variation dB_z/dt caused by the current flow re-distribution in the cable away from the normal zone

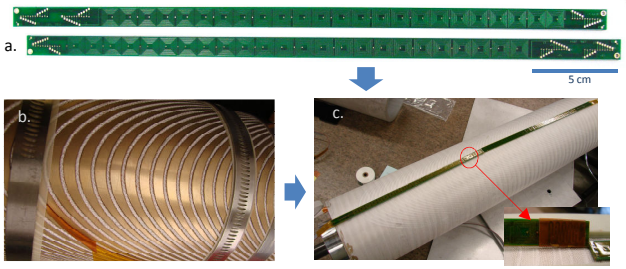

Fig. 2. (a) PCB antenna arrays as-fabricated. (b) Top view of the CCT magnet outer layer winding: NbTi cable is inserted in the groove of the Al bronze mandrel.(c) Quench antenna arrays placed along the CCT magnet pole, atop of the cable winding. Inset – heater mounted at the end of one array to initiate quenches in the magnet.

Four arrays were installed on the outer layer of the CCT NbTi magnet, two per each pole side facing the winding as shown in Fig 2 a-c. They were later secured with G10 cylindrical spacers, and epoxy-impregnated with the coils. The antenna signals were acquired simultaneously with coil voltages by the MTF DAQ system at 400 kHz, in a time window of up 1 s centered around the quench trigger time.

Cryogenic amplifier / multiplexer

To facilitate interfacing of multiple sensor arrays and reduce cryostat wiring we developed a cryogenic multiplexer/preamplifier based on CMOS IC elements. Schematic of the device is shown in Fig. Two 8-channel DG407 analog multiplexers are commutating 16 differential inputs to a gain x50 amplifier built using ICL7611 op-amp.

Cryogenic operation of similar CMOS ICs has been earlier discussed in [2]. LabView software interface on a PC was used to program the input sequence through En&A0-A2 terminals with TTL-level control signals and to digitize the amplified analog output. Supply voltage of the multiplexer is auto-adjusted upwards upon cooldown by employing temperature-dependent voltage breakthrough characteristics of DZJ062 Zenner diodes. IC elements were protected with GE Silicone II sealant to reduce thermal

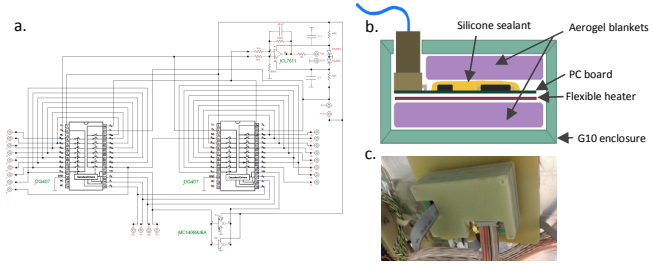

Fig. 3. (a) Schematic of the cryogenic multiplexer/amplifier. (b) cross-section of the enclosure box. (c) multiplexer mounted at the bottom surface of the cryostat thermal shield.,Il;

shock. Initially, the board was installed in the upper portion of a cryostat and cooled with helium gas from the pressurized liquid helium Dewar. Reliable operation has been confirmed down to 30 K, with switching rates up to 60 kHz/ch limited by the performance of control software. At lower temperatures the DG407 ICs were no longer responding to control voltages, but the operation restored back to normal at above 30 K. To extend low-temperature functionality, the board was sandwiched with a flexible Kapton sheet incorporating a 50-micon thick stainless heater (R = 9 Ω) and two Aerogel blankets inside a G10 box enclosure. Preliminary tests indicated that with 0.3 A dc current in the heater the board temperature can be raised above 30 K without having any notable impact on the helium boil-off rate. Further tests are in progress.

Acoustic quench localization system

Acoustic emission sensing is a technique allowing for various advanced quench diagnostics to be done in no-invasive way through sensing and timing acoustic signals emitted prior and during quenching. Normally, impregnated magnets emit a strong acoustic "burst" just prior to quenching caused by mechanical fracture and/or sudden local heat dissipation at the conductor. By precise timing of sound wave arrival to the sensors installed at the magnet surfaces, location of the acoustic emission source can be determined. Our system is based on amplified cryogenic piezoelectric sensors allowing for quench localization with ~ 5 cm accuracy. The integrated preamplifier with gain of

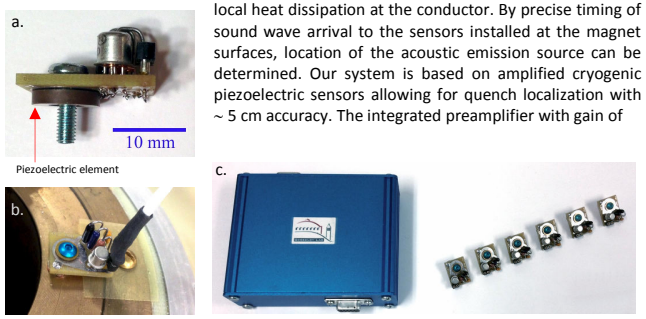

Fig. 4. (a) Acoustic emission sensor (side view). (b) Sensor installed the end of a CCT magnet (two sensors at the opposite ends were installed) (c) Components of a six-sensor acoustic quench localization system built for future studies.

~ 5-10 is constructed using a GaAs FET operating reliably at liquid helium temperatures. It down-converts impedance of the piezo-element for a dramatic improvement in signal to noise ratio. Details of sensor electronics and calibration are given in [3]. Sensors are attached to the magnet structure using a single screw. Signals are digitized at 1 MHz for quench localization purpose using Yokogawa WE7000 DAQ.

Examples of quench localization and magnet diagnostics

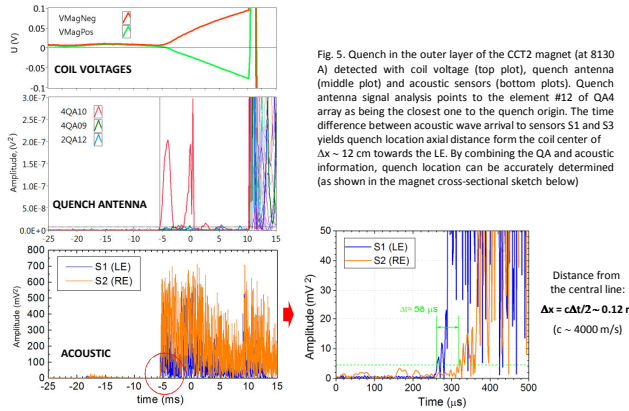

Fig. 5. Quench in the outer layer of the CCT2 magnet (at 8130 A) detected with coil voltage (top plot), quench antenna (middle plot) and acoustic sensors (bottom plots). Quench antenna signal analysis points to the element #12 of QA4 array as being the closest one to the quench origin. The time difference between acoustic wave arrival to sensors S1 and S3 yields quench location axial distance form the coil center of Δx ~ 12 cm towards the LE. By combining the QA and acoustic information, quench location can be accurately determined (as shown in the magnet cross-sectional sketch below)

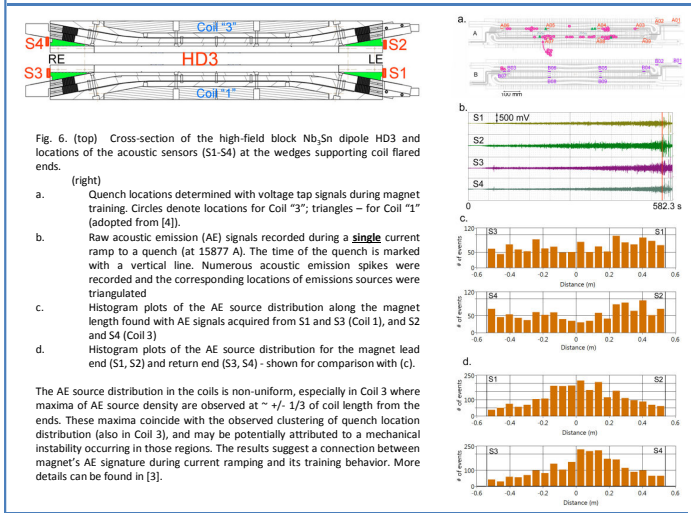

Fig. 6. (top) Cross-section of the high-field block Nb_3Sn dipole HD3 and locations of the acoustic sensors (S1-S4) at the wedges supporting coil flared ends.

(right)

a. Quench locations determined with voltage tap signals during magnet training. Circles denote locations for Coil "3"; triangles – for Coil "1" (adopted from [4]).

b. Raw acoustic emission (AE) signals recorded during a **single** current ramp to a quench (at 15877 A). The time of the quench is marked with a vertical line. Numerous acoustic emission spikes were recorded and the corresponding locations of emissions sources were triangulated

c. Histogram plots of the AE source distribution along the magnet length found with AE signals acquired from S1 and S3 (Coil 1), and S2 and S4 (Coil 3)

d. Histogram plots of the AE source distribution for the magnet lead end (S1, S2) and return end (S3, S4) - shown for comparison with (c).

The AE source distribution in the coils is non-uniform, especially in Coil 3 where maxima of AE source density are observed at ~ +/- 1/3 of coil length from the ends. These maxima coincide with the observed clustering of quench location distribution (also in Coil 3), and may be potentially attributed to a mechanical instability occurring in those regions. The results suggest a connection between magnet's AE signature during current ramping and its training behavior. More details can be found in [3].

References

[1] S. Caspi, L. Brouwer, T. Lipton, A.R. Hafalia Jr., S. Prestemon, D.R. Dietderich, H. Felice, X. Wang, Rochepault, A. Godeke, S. Gourlay, M. Marchevsky, *"Design of an 18-T Canted Cosine-Theta Superconducting Dipole Magnet"*, IEEE Trans. Appl. Supercond. 25, 4000205 (2015), DOI: 10.1109/TASC.2014.2360354

[2] S. V. Uchaikin, P. Christ, F. Probst, S. Rutzinger, W. Sedel, *"Fast cryodetector and SQUID read-out for mass spectrometry"*, Physica C 367, 295-297 (2002). E.D. Buchanan, D. J. Benford, J. B. Forgione, S. H.Moseley , E. J. Wollack, *"Cryogenic applications of commercial electronic components"*, Cryogenics 52, 550-556 (2012)

[3] M. Marchevsky, G. Sabbi, H. Bajas, S. Gourlay, *"Acoustic emission during quench training of superconducting accelerator magnets"*, Cryogenics 69, 50-57 (2015), DOI: 10.1016/j.cryogenics.2015.03.005

[4] M. Marchevsky, S. Caspi, D. W. Cheng, D. R. Dietderich, J. DiMarco, H. Felice, P. Ferracin, A. Godeke, A. R. Hafalia, J. Joseph, J. Lizarazo, P. K. Roy, G. Sabbi, T. Salmi, M. Turqueti, X. Wang, S. Prestemon, *"Test of the High-Field Nb_3Sn Dipole Magnet HD3b"*, IEEE Trans. Appl. Supercond. 24, 4002106, (2014) DOI: 10.1109/TASC.2013.2285881